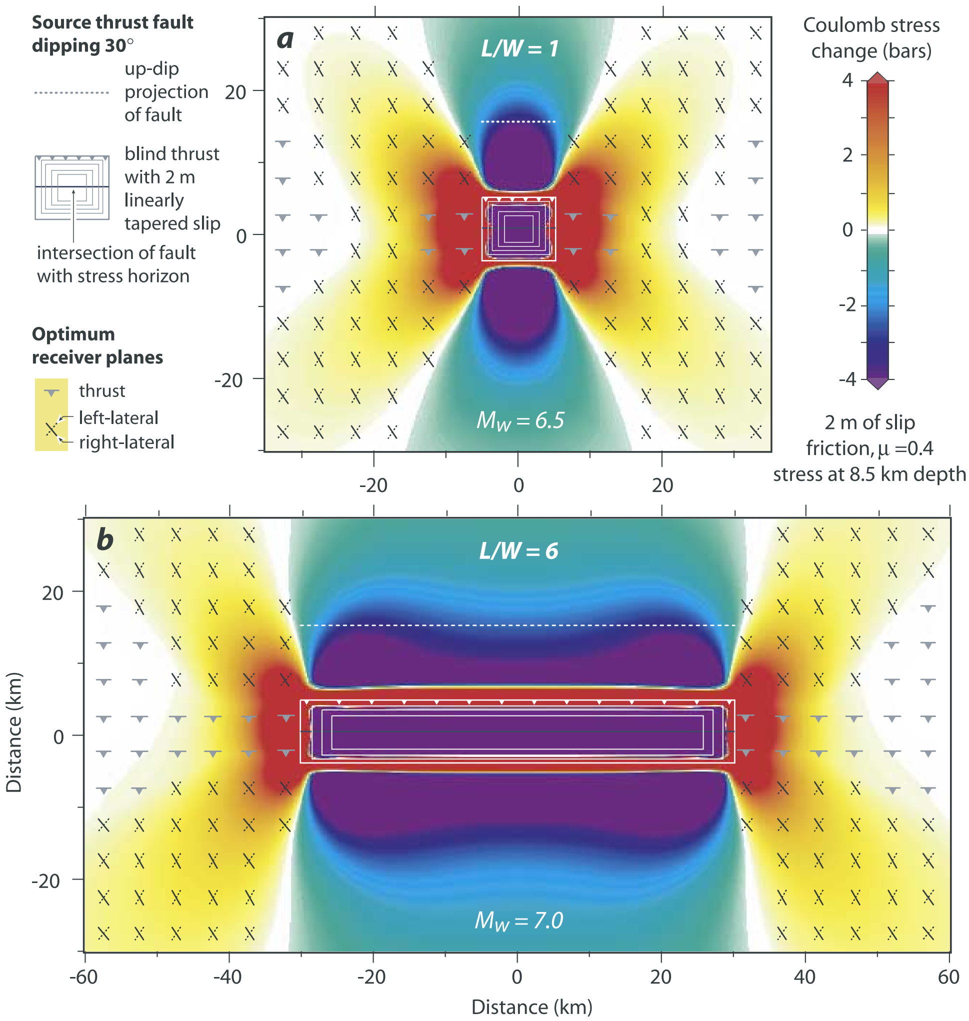

Figure 4. Stress transferred by (a) short versus (b) long blind thrust source faults dipping 30°. Stress is sampled on a horizontal plane bisecting the fault. To illustrate which type of receiver fault is most likely to be promoted, stress is calculated on optimally oriented receiver faults; in other words, at every point the plane on which the Coulombs stress change is most positive is shown. The stress increases beyond the ends of the long and short source fault are about the same, but the zone of stress decrease perpendicular to the strike of the source fault is much broader along strike for the long fault. While thrust faulting is promoted beyond the ends of a thrust fault rupture, the region over which strike-slip faulting is enhanced extends over a much larger area.

ruptures are efficient in inhibiting thrust faults in a large region perpendicular to the rupture plane.

3. Stress Transfer in a Continental Blind Thrust Sequence

[13] The central California Coast Ranges suffered a southeast propagating sequence of blind thrust earthquakes that includes the 1982 M_w = 5.8 New Idria, 1983 M_w = 6.7 Coalinga, 1983 M_w = 6.0 Nuñez, and 1985 M_w = 6.0 Kettleman Hills earthquakes. The main shocks were separated by 8, 2, and 25 months, respectively. In keeping with most studies, we treat the events as occurring on west dipping thrust faults, although it should be noted that *Dickinson* [2002] argues that the shocks most likely struck on east dipping reverse faults. Although stress transferred by the New Idria to the Coalinga shock is negligible (Figure 7a), the stress imparted by the Coalinga event to the Nuñez rupture plane is large (Figure 8), suggesting that the Coalinga shock promoted the Nuñez earthquake. The Coulomb stress increase at the base of the Nuñez fault is about 4–10 bars (Figures 8a and 8b), and is unclamped by 20 bars, because of its proximity to the Coalinga source (Figure 8d).

[14] Aftershocks of the New Idria and Coalinga events are concentrated in regions of calculated Coulomb stress increase (Figures 7a and 7b), although this is less true for the Kettleman Hills aftershocks (Figure 7c). In cross section, the distributed pattern of Coalinga aftershocks in the epicentral area (Figure 9b) and at the future epicenter of the Kettleman Hills shock (Figure 9c) is also in rough accord with the calculated Coulomb stress change. The absence of such correlations between background seismicity and the subsequent earthquake stress changes (Figures 7d–7f and Figures 9d–9f) furnishes additional support that after-